Pure Appl. Geophys. 178 (2021), 1943–1957

https://doi.org/10.1007/s00024-021-02737-8

Pure and Applied Geophysics

Application of Signal Processing in Tracking Meteorological Drought in a Mountainous Region

Babak Vaheddoost[1] and Mir Jafar Sadegh Safari[2]

Abstract—This study addresses the application of signal processing in the evaluation of meteorological drought associated with monthly precipitation time series. Several drought indices and a Haar wavelet decomposition (WD) with ten components are implemented in the evaluation of the monthly precipitation of a mountainous region called Mount Uludag in Turkey. Monthly precipitation time series in three meteorological stations at the summit and foothills are used. The Standardized Precipitation Index (SPI) is used at monthly, annual, and 12- and 48-month moving average time frames as the benchmark to investigate the drought patterns. The results obtained by the WD and SPI are then confirmed using the *Z*-score index (ZSI) at monthly and annual scales, together with the modified China *Z*-index (MCZI) and rainfall anomaly index (RAI) at a monthly scale. Changes in the moments of the distribution, correlation analysis, mutual information, and power spectrum are applied to investigate the nature of the relationship between the sequences of precipitation events in time and space. The temporal correlation analysis, together with the mutual information, showed that the system has a short-term memory with strong seasonality. Similarly, the power spectra depicted major seasonality at 1, 3, 5, 6, 12, 22, and 60 months in the precipitation time series. It is concluded that the recent drought events have an infrequent nature, which altered the sinusoidal patterns of the large-scale events. The SPI-48 and the WD showed that declines are strongly related to the large-scale cycles, but the decline patterns are more related to the station located at the mountain summit.

Keywords: Drought, Mount Uludag, RAI, signal processing, SPI, *Z*-score.

1. Introduction

Droughts are complicated phenomena, and it is difficult to identify a common definition of their drivers and consequences. All droughts start with a deficit in precipitation in time or space and develop into a more complicated hydrometeorological situation. Drought events are studied under five major classes of (1) meteorological, (2) agricultural, (3) hydrological, (4) socioeconomic, and (5) ecological (Yihdego et al., 2017). These classes respectively indicate the reduction in precipitation, lack of moisture in the soil, decline in stream-flows, shortage in water required to meet human needs, and water deficit in biota (Yihdego et al., 2017, 2019). Many indices and indicators have been developed to measure, define, and/or forecast drought events (e.g. Mehdizadeh et al., 2020; Mehr et al., 2021; Wilhite & Glantz, 1985; Yihdego et al., 2019).

An index is a method of deriving value-added information linked to drought by comparing current conditions with historical events (Eslamian, 2014; Hao & Singh, 2015; Azmi et al., 2016). To this end, the World Meteorological Organization (WMO) investigated the applicability of a single index to provide a standard methodology in the evaluation of meteorological drought. The Standardized Precipitation Index (SPI) was selected as the most effective single variable index which can be evaluated for this aim. Even before the WMO (2011), the SPI received considerable attention in tracking drought conditions. The SPI was developed by McKee et al. (1995) and used continuously in the relevant literature (e.g. Rashid & Beecham, 2019; Starks et al., 2019; Vaheddoost, 2019). Alternative indices have been developed to address drought in different ways. These include the rainfall anomaly index (RAI; Van Rooy, 1965), deciles index (DI; Gibbs & Maher, 1967), Bhalme and Mooley drought index (BMDI; Bhalme & Mooley, 1980), percent of normal precipitation index (PNPI; Willeke et al., 1994), *Z*-score

[1] Department of Civil Engineering, Bursa Technical University, Bursa, Turkey. E-mail: babak.vaheddoost@btu.edu.tr
[2] Department of Civil Engineering, Yaşar University, Izmir, Turkey. E-mail: jafar.safari@yasar.edu.tr

index (ZSI; Edwards & McKee, 1997), China *Z*-index (CZI; Ju et al., 1997), and Standardised Precipitation-Evapotranspiration Index (SPEI; Vicente-Serrano et al., 2010). Indices or indicators are developed based on the preliminary needs and to address the spatial and/or the temporal behavior of droughts across the globe (Yihdego et al., 2017).

Mountainous regions or highlands have particular climatic behavior which is strongly connected to the geomorphology and orientation of the terrain. Numerous studies have investigated the effect of climate events on drought, including those conducted in China (e.g. Gao & Zhang, 2016; Li et al., 2020; Sun et al., 2019), Jordan (e.g. Aladaileh et al., 2019), Iraq (e.g. Jasim & Awchi, 2020), Iran (e.g. Bahrami et al., 2019; Sharafati et al., 2020), Peru (e.g. Mohammadi et al., 2020; Vaheddoost, 2020a), Syria (e.g. Mohammed et al., 2020), and Turkey (e.g. Afshar et al., 2020; Cavus & Aksoy, 2019; Eris et al., 2020; Sen et al., 2012; Turkes, 2020). As mountainous regions have a great influence on the regional climate, it is important to investigate the effect of climate-born events on droughts. For instance, Du et al. (2013) used SPI with different time spans to address extreme rainfall events in the context of climate change in Hunan Province, China. The correlation coefficient between the discharge of rivers and SPI time series was investigated and it was concluded that the area is becoming drier in spring and autumn, while summer and winter are becoming wetter. Zhu et al. (2016) used spatial and temporal analysis to evaluate drought in Hengduan Mountains, China. Data records at 26 meteorological stations for the time period 1960–2012 were used to calculate the Φ index (calculated as a vertical line drawn on the hyetograph in which the total area between the Φ and the hyetograph is equal to the runoff depth) calibrated by the Penman–Monteith modification. Results indicated that a shift occurred, and the sub-humid conditions were replaced by humid conditions. Analysis indicated an increasing trend in summer and autumn, while the drought index was found to be inversely proportional to the relative humidity of the soil and normalized difference vegetation index. More recently, studies were conducted by Hao et al. (2019, 2020), Zhou et al. (2019), and Craig et al. (2020) to investigate the effect of climate-born events on the drought patterns in mountainous regions. There is a vast body of literature about Mount Uludag, which is a tourist destination and an important snowpack reservoir. Accordingly, prior studies conducted by Turkes et al. (2007), Ozturk (2010), Sen (2013), Tatli (2015), Yilmaz (2018), Katip (2018), and Vaheddoost (2019) can be suggested for further investigation. Based on these studies, the recent decline in the precipitation time series at the summit of Mount Uludag can be linked to climate change or climate variability. Vaheddoost (2020b) concluded that the climatic events of recent years (i.e. 2016–2018) were linked to the low-frequency events with high magnitudes and were more likely to be linked to climate variability than climate change. Although the time series used for the analysis was less than 30 years, it was found that the temporal changes could be evaluated using the probability distribution function. Similarly, trends associated with the precipitation time series were found to be decreasing (Sen, 2013; Simisek & Cakmak, 2010; Sirdas & Sen, 2003), which can be interpreted as an initiation of a long-lasting drought. Hence, these studies indicated that the trends are slightly significant; however, the scale of high-magnitude events together with the sinusoidal oscillation in the time series needs to be properly investigated.

This study aims to investigate the drought events at Mount Uludag using signal processing and drought indices associated with the precipitation records. For this, drought events are examined using (1) the SPI, ZSI, modified CZI [MCZI], and RAI drought indices together with the (2) wavelet decomposition at three stations located at the summit and downhill of Mount Uludag. The results obtained were compared with each other to determine whether the identified events were exclusive to a method or a set of real events.

2. *Study Area and Data*

The study area covers the summit and northern and southern hillsides of Mount Uludag in Bursa district, northwestern Turkey. The summit of this mountain is the highest elevation in the Marmara region (2543 m above sea level), while the hillside is almost at sea level. The orientation of the mountain is

about 40 km from west to east and 15–20 km from north to south. Since Uludag is a major player in the hydrology of the Bursa (Vaheddoost, 2020b), any drought can endanger the water and food security in the region. Based on the Köppen–Geiger climate classification, it has a mild temperate climate with dry/cool summers. The total annual precipitation is as high as 704 mm, and the average annual temperature is about 14.6 °C. Monthly precipitation data recorded in Uludag station (40.107 E; 29.129 N; 1877 m above sea level) near the summit, together with the data records at Keles (39.915 E; 29.231 N; 1063 m above sea level) and Osmangazi (40.231 E; 29.013 N; 100 m above sea level) stations located at the hillside of Mount Uludag, are used in the study (Fig. 1). The data for the time period of January 1980 to October 2018 were acquired from Bursa State Meteorological Service. The statistical properties of the provided time series are given in Table 1. The mean monthly precipitation records were tested for consistency, existence of trends, and outliers (Vaheddoost, 2020b). The results showed that precipitation is highly variable, and the probability distribution function is positively skewed in all

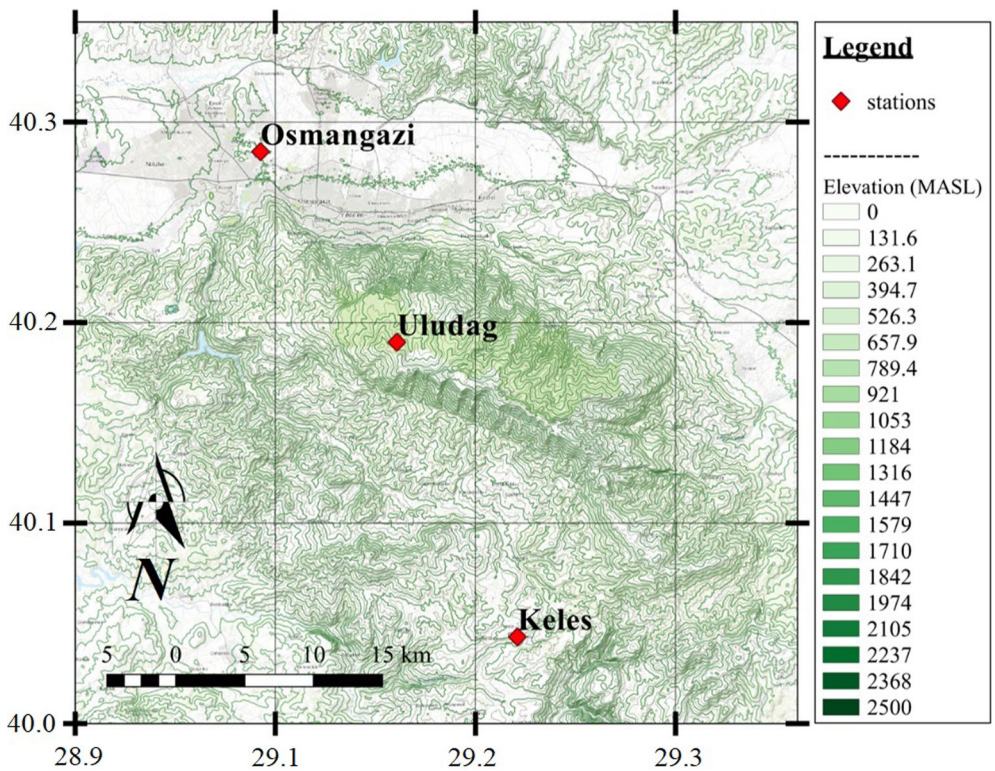

Figure 1
Bursa map and location of the selected stations

Table 1

Statistical properties of precipitation time series at the selected stations

Station	ID	Mean (mm)	Standard deviation (mm)	Coefficient of variation	median (mm)	Skewness	Kurtosis	Maximum (mm)
Uludag	ULU	119.63	101.40	0.84	97.30	2.17	15.25	1000
Osmangazi	OSM	59.97	47.98	0.80	50.95	1.38	7.78	397
Keles	KEL	60.98	48.64	0.79	48.95	1.06	3.98	254

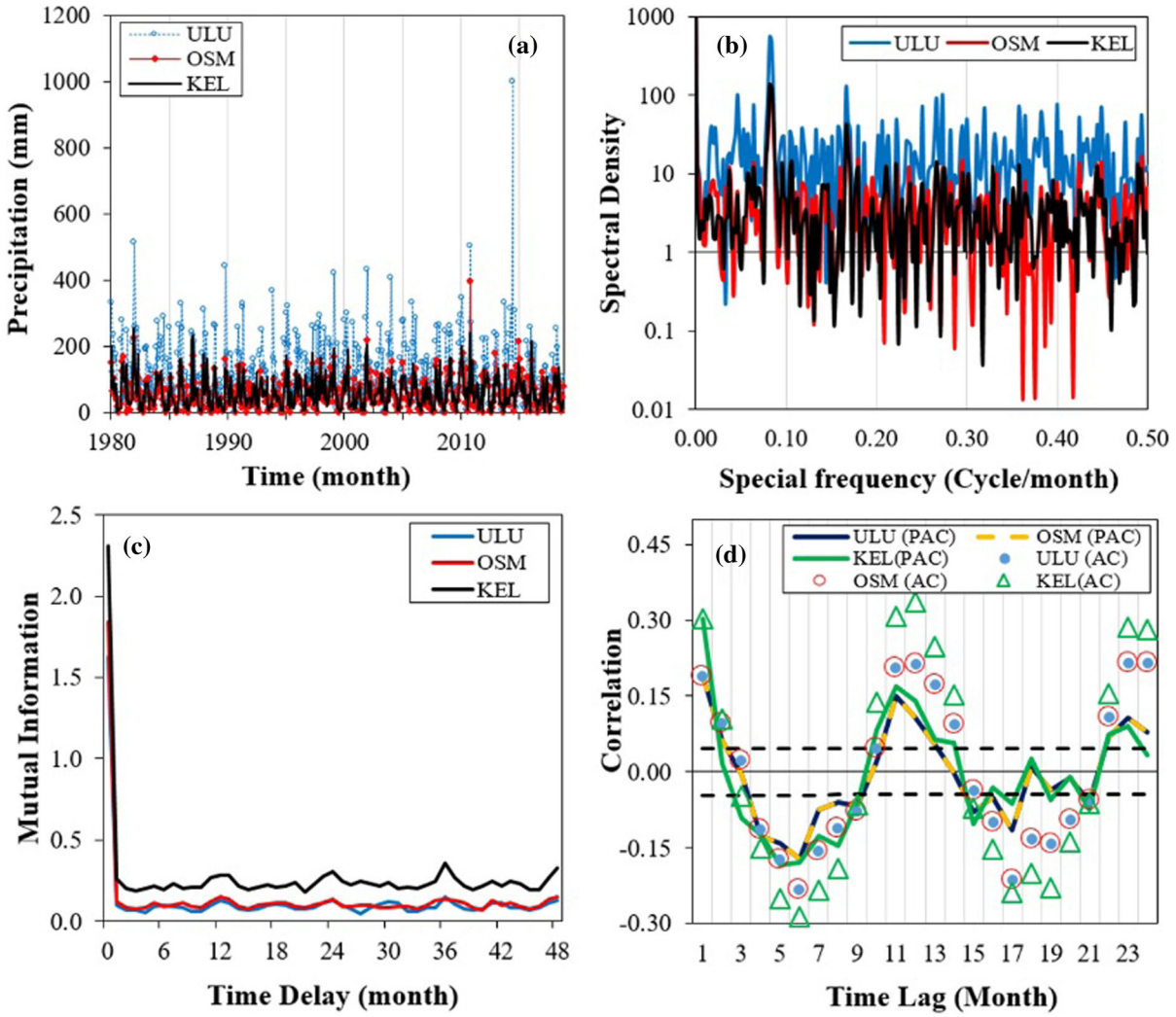

Figure 2
Signal analysis including **a** time series plot, **b** power spectrum, **c** mutual information, **d** correlation analysis of the precipitation time series at the selected stations

stations. The maxima reach 1000 mm/month (i.e. extreme event; see Fig. 2a), and the kurtosis is highly leptokurtic. The stations at the hillside show similar statistics, while the kurtosis at Osmangazi is higher than the other stations. The Uludag station has the highest mean precipitation, which can be linked to the orographic precipitation at high altitudes. In the remaining parts of this study, the monthly precipitation time series are used in the signal processing and defining the different drought indices for further discussion.

3. Methodology

To evaluate the drought patterns in the selected stations, wavelet decomposition and drought indices are used. Results are interpreted as the evidence for the real events which are confirmed by the set of different methods used in this study. This would help to understand the nature of the precipitation and drought events in the study area as well as the applicability of various indices in the mountainous region.

3.1. Signal Processing Analysis and Properties of the Data

Signal processing is the ensemble of methods that are applied to the data, considered either at time or frequency domains for temporal or spatiotemporal analysis. This study searches for the presence of deterministic (e.g. trend, seasonality, cycles) and/or stochastic (e.g. auto-correlation, partial auto-correlation, self-similarity, power spectrum, mutual information, entropy) events to interpret the behavior of the precipitation time series in the region. For this, the auto-correlation (AC), partial auto-correlation (PAC), mutual information (MI), power spectrum (PS), wavelet decomposition (WD), and moments of the probability distribution are used to investigate the properties of the monthly precipitation time series.

3.1.1 Correlation Analysis

The correlation analysis defines the dependence of two independent events in time and/or space. In this regard, autocorrelation can be introduced as the temporal linear correlation of the time series with itself at different time lags. It can be introduced as

$$\rho_k = \frac{\sum_{t=1}^{n}(x_t - \overline{x})(x_{t-k} - \overline{x})}{\sum_{t=1}^{n}(x_t - \overline{x})^2}, \quad (1)$$

while the kth lag of the AC function with value of ρ can be estimated by the observed values of the time series x_t for $t = 1, \ldots, n$. The PAC can be expressed as the AC when the components of the function are independent of each other. Therefore, the combination of AC and PAC is used to interpret the systematic cycles and persistence in the time series in particular when autoregressive integrated moving average models are needed. More details about the application of the autocorrelation coefficient in time series analysis may be found in Kashyap and Rao (1976) and Salas et al. (1980).

The mutual information (MI; Gray, 1990) and the related function can be used to interpret the conditional and temporal relations simultaneously. It is based on the probability and the information entropy (Shannon & Weaver, 1949), which can be expressed as

$$I(X_t, X_{t-k}) = \sum_{x_t, x_{t-k}} P(x_t|x_{t-k}) \log \frac{P(x_t|x_{t-k})}{P(x_t)P(x_{t-k})}, \quad (2)$$

in which the joint probability $P(x_t|x_{t-k})$ of the temporal outcome is evaluated. Several consecutive lags are then calculated, and the first minimum associated with the mutual information function is used as a milestone in the analysis.

3.1.2 Spectral Analysis

The power spectrum evaluation is based on the Fourier transformation function. It uses a softening window (here, Tukey window) for transforming the line spectrum to the power spectrum and can be expressed as

$$x_t = \mu + \sum_{k=1}^{\frac{N}{2}} [\alpha_k \cos(2\pi f_k t) + \beta_k \sin(2\pi f_k t)] + \varepsilon_t, \quad (3)$$

where μ is the mean value of the time series which is considered to be zero when the time series has previously been standardized for the analysis; ε is the random component of the time series; α and β are Fourier coefficients; and k is the number of items in the time series. The upper bound of the summation is set at $(N - 1)/2$ if N (in this study, 466) is an odd number. Then, the significant frequencies which show different spikes can be used to obtain the most important repeating periods in the time series by taking the reverse of the obtained frequencies. The interested reader may refer to Rader and Brenner (1976) and Kashyap and Rao (1976) for more details about fast Fourier transformation and spectral analysis.

3.1.3 Wavelet Decomposition (WD)

Wavelet decomposition is a method used to determine a time series as a signal, composed of several signals. A Haar wavelet decomposition for S_t can be defined as

$$S_t = a_i + \sum_{i=0}^{m} d_i, \quad (4)$$

where a is the trend or moving average (linear or nonlinear representation of the sample mean) and d_i is the ith harmonic used in decomposition. It is

demonstrated that the signal S is the result of the sum of a_n and $d(s)$, achieved by the decomposition of the allocated signals (in this study n: 10). Each component (obtained signal) is then used to interpret the phenomenon and its link to different events. For instance, a signal of wider frequency may indicate large-scale climatic events such as climate change and climate variability. On the other hand, a signal with low frequency can be interpreted as the random nature or the passiveness of the events in the time series. The magnitude of those events, however, defines the effectiveness of the signal which is used in the study. The interested reader may refer to Meyer (1992) for more details.

3.2. Drought Indices

Drought indices are a simple approach for evaluating droughts compared to the sophistical hydrometeorological models and field measurements. When the meteorological drought is investigated, the drought indices with one variable (i.e. predictor) are the most practical way of studying droughts in the presence of outliers, missing data, and short data records. The SPI at monthly and annual scale together with 24 and 48 months moving average are used in the analysis. Alternatively, ZSI at monthly and annual scale together with MCZI and RAI indices at monthly scale are used to be compared to the results obtained by the signal processing.

3.2.1 Standardized Precipitation Index (SPI)

The SPI developed by McKee et al. (1995) is used in evaluating droughts based on the precipitation time series. The SPI is calculated by fitting precipitation data to a gamma distribution (Caloiero & Veltri, 2019; Abramowitz & Stegun, 1970). Accordingly, different time spans are used to obtain an SPI value which is used in defining the type and severity of the droughts. Table 2 shows the criteria used to evaluate these values (WMO, 2011). Additionally, different time spans are used in the analysis to evaluate the degree and class of drought severity. For instance, a 1-month SPI evaluation (SPI-1) is an indicator of the deficit or surplus of the precipitation in the region, while 12- (SPI-12) and 48-month (SPI-48) moving average SPIs are used respectively to project the drought effect on the reservoir and climate of the region (Sepulcre-Canto et al., 2012; Yihdego et al., 2019). To calculate the values of the SPI in this study (reference period 1980–2018), MDM [Meteorological Drought Monitor] free software was used (AgriMetSoft, 2017). It is worth noting that more recent and/or sophisticated drought indices such as the SPEI can also be used in the analysis if more than one parameter is used in the evaluation.

Table 2

SPI evaluation criteria (WMO, 2011)

SPI values	Condition
SPI $\geq$ 2.0	Extremely wet
2.0 > SPI $\geq$ 1.50	Very wet
1.50 > SPI $\geq$ 1.00	Moderately wet
0.99 > SPI $\geq$ -−0.99	Near normal
−1.00 > SPI $\geq$ −1.49	Moderately dry
−1.50 > SPI $\geq$ −1.99	Severely dry
SPI $\leq$ −2.0	Extremely dry

3.2.2 Z-Score Index (ZSI)

This index is as simple as SPI, but it does not need any adjustment for the data or being fitted to a predefined distribution function such as gamma or Pearson type III. It can be obtained by dividing the residual of precipitation and mean precipitation by the standard deviation of the sample time series. Based on previous studies, the Z-score is incapable of depicting the properties of the drought in time series of short records (Edwards & Mckee, 1997), while in practice it is comparable to the other indices. Accordingly, Table 3 shows the criteria used in

Table 3

ZSI evaluation criteria (WMO, 2011)

ZSI values	Condition
ZSI $\geq$ 0.25	No drought
0.25 > ZSI $\geq$ −0.25	Weak drought
−0.25 > ZSI $\geq$ −0.52	Slight drought
−0.54 > ZSI $\geq$ −0.84	Moderate drought
−0.84 > ZSI $\geq$ −1.25	Severe drought
ZSI < −1.25	Extreme drought

evaluating the ZSI in application (WMO, 2011). In this study, the index was used at monthly and annual scales, simultaneously. To calculate the values of the ZSI, MDM software was used (AgriMetSoft, 2017).

3.2.3 Modified China Z-Index (MCZI)

The CZI and the modified China *Z*-index were suggested by the National Climate Center of China in 1995 as a regional alternative to the well-known SPI (Ju et al., 1997), whilst the long-run mean of the precipitation time series can be fitted to a Pearson type III distribution. The CZI uses the Wilson-Hilferty cube-root transformation (Wilson & Hilferty, 1931). Table 4 shows the criteria used in the evaluation of the CZI or MCZI in the analysis (WMO, 2011). In the present study, the MCZI at monthly scale was used due to the limitation of the MDM and its applicability in confirmation of the SPI and ZSI.

3.2.4 Rainfall Anomaly Index (RAI)

The RAI (Van Rooy, 1965) or the modified RAI uses a ranking procedure to assign magnitudes to anomalies (i.e. positive and negative anomalies) in the precipitation time series. For this, the precipitation data are ranked in descending order. The ten values with the highest magnitudes are then averaged to obtain a threshold for the positive anomalies, while the ten values with the lowest values are averaged to obtain a threshold for the negative anomalies. Table 5 shows the criteria used in the analysis of the RAI in the application (WMO, 2011). Accordingly, the RAI was evaluated at a monthly scale due to the limitation of MDM and its applicability in confirming the SPI and ZSI.

Table 4

MCZI evaluation criteria (WMO, 2011)

MCZI values	Condition
MCZI > 2	Extremely wet
$1.5 <$ MCZI ≤ 1.99	Very wet
$1.0 <$ MCZI ≤ 1.49	Moderately wet
$-0.99 <$ MCZI ≤ 0.99	Near normal
$-1.0 <$ MCZI ≤ -1.49	Moderately dry
$-1.5 <$ MCZI ≤ -1.99	Severely dry
MCZI < -2	Extremely dry

Table 5

RAI evaluation criteria (WMO, 2011)

RAI values	Condition
RAI ≥ 0.3	Extremely wet
$0.3 >$ RAI ≥ -0.3	Moderately wet
$-0.3 >$ RAI ≥ -1.2	Near normal
$-1.2 >$ RAI ≥ -2.1	Moderately dry
$-2.1 >$ RAI ≥ -3.0	Severely dry
RAI < -3.0	Extremely dry

4. Results

Based on the methodology detailed above, first, the signal of the precipitation time series was evaluated. The aim is to trace patterns, anomalies, similarities, and deviations in the data run. For this, data were checked for inconsistencies and data loss. According to Vaheddoost (2020b), the time series of the precipitation at the selected stations and the time period of 1980–2018 were consistent, and there were no significant short-term trends in the data run. However, the precipitation time series at Mount Uludag seems to have experienced a sudden drop in recent years. Figure 2a shows the precipitation time series of the Uludag stations between 1980 and late 2018. There is an extreme record in early 2015 at ULU station which reaches 1000 mm/month. The precipitation time series at the OSM and KEL, however, are similar and do not show major differences. The 2015 event at ULU (Fig. 2a, the extreme event) is expected to depict a wet period for some time in the drought patterns. Following the time series (Fig. 2a) in Fig. 2b, the power spectrum of the seasonality is given. In general, the magnitude of the seasonal events is stronger in ULU, while the OSM shows the lowest frequency. The highest peaks of all stations are located at 0.16, 0.08, and 0.05 periodicities, which correlate with 6-month, 11.9-month ($\sim$ 1 year), and 21.3-months ($\sim$ 2 years) periodicity, respectively. There are also significant spikes at each 1, 3, 5, 60 months that can be evaluated

separately. Large-scale cycles also reach to infinity, which are ignored in this study. In Fig. 2c on the other hand, the mutual information function of the signal is given. Since the first minimum at ULU is located at lag 3, it plays an important role in the seasonal persistence. The MIF at the OSM is also located at the third lag, while the KEL showed that the fourth lag has the lowest minima. This might be linked to the delayed effect of the air front that passes through the mountain hills from north to south. The correlation analysis in Fig. 2d more precisely shows that the phenomena have low memory, as expected (i.e. the random nature of the precipitation). The ULU and OSM stations show similar behavior, while the correlation patterns at KEL are different (Fig. 2c, d) which might be linked to the air fronts passing through the high elevation. Although the sinusoidal patterns at both AC and PAC are partly disturbed, it shows that a moving average (MA) can be useful in the evaluation of the time series. In brief, the nature of the monthly precipitation at the stations is of the cyclic type, which eventually alters the climate of the surrounding area. The oscillatory nature of the phenomenon, however, is very useful when a long-lasting event such as drought is studied. Therefore, the historical drought events at Uludag followed by a surplus can be interpreted as natural consequence of extreme events. Similarly, the high magnitude of the spike in the power spectrum shows that there is at least one large frequency that has a major effect on the phenomenon. This can be interpreted as the effect of climate change or climate variability on the regional climate.

Results of WD of the precipitation time series at the selected stations are given in Fig. 3. Based on the results, the $a8$ pattern at ULU depicts a major decline in recent years. A similar pattern with lower significance is also observed in the KEL station, but the OSM shows consistent behavior. In other words, the decline in precipitation at the mountain peak is observed at the southern hillside, which is quite reasonable. Since a is not a harmonic component, the evidence of trend at ULU is obvious and can be extended to KEL stations as well. The remaining decomposed signals showed a more oscillatory nature. Particularly in $d3$, $d7$, and $d8$, a cyclic behavior is observed. In other components including but not limited to $d1$ and $d2$, a repeating pattern at different magnitudes showed that the attractors of the system are quite stable. This may be linked to the natural drivers of the precipitation in the region. It may be due to a larger seasonality, which is explained in Fig. 2b (i.e. the power spectrum). The disturbance in 2015 for ULU is of the random kind, which is ignored in the pattern analysis. Since the length of data is 465 months, it is difficult to determine whether larger harmonics are the main reason for the decline at ULU. However, the similar decline in KEL and consistency in OSM shows that the changes are of the local type or linked to the orographic precipitation.

The precipitation time series were divided into five time spans of 1980–1987, 1988–1995, 1996–2003, 2004–2011, and 2012–2018 to be used in distribution analysis (Fig. 4a–c). Vaheddoost (2020b) suggested that the investigation of the changes in the probability distribution is very handy in identifying the magnitude and frequency of undetected trends and outliers in the precipitation time series. Figure 4 illustrates the temporal changes in the distribution during the study period using box-plots. It is shown that the kurtosis of the data in ULU is continuously decreasing and the distribution of the monthly precipitation is becoming more platykurtic, which indicates that the recent precipitation events are less frequent compared to the historical records. Considering the outliers in the data, it is obvious that the magnitude of the extreme events in ULU has increased. On the contrary, the outliers associated with the OSM and KEL stations experienced a decrease. As illustrated, the gradual decline in the precipitation can be an early warning for the upcoming drought events, which may linger for quite a length period in the region. When the pattern recognition is considered, the decomposed signals of $d4$ and $d7$ at ULU showed that the return period between events is decreasing, and this may be due to the changes in the climatic events. The link between KEL and ULU stations also confirms that the decline in precipitation in the summit extends to the southern hillside. Additionally, when the decomposed patterns at ULU are compared to those of OSM and KEL stations, it is reasonable to conclude that the nature of the events at ULU is oscillatory and showed large variations. In this respect, drought patterns at ULU

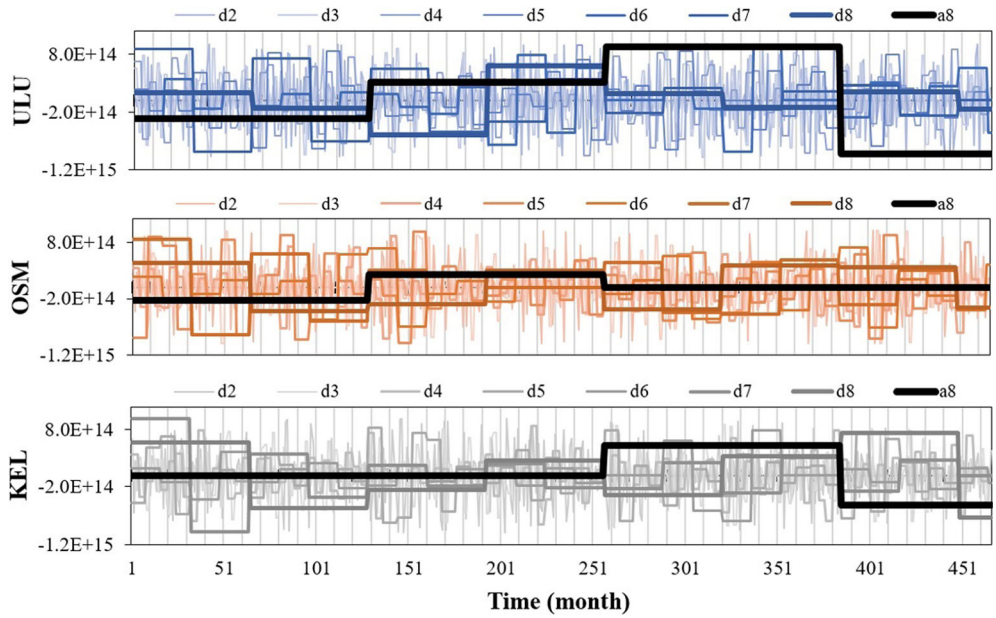

Figure 3
Components of the precipitation time series at the selected stations obtained by WD

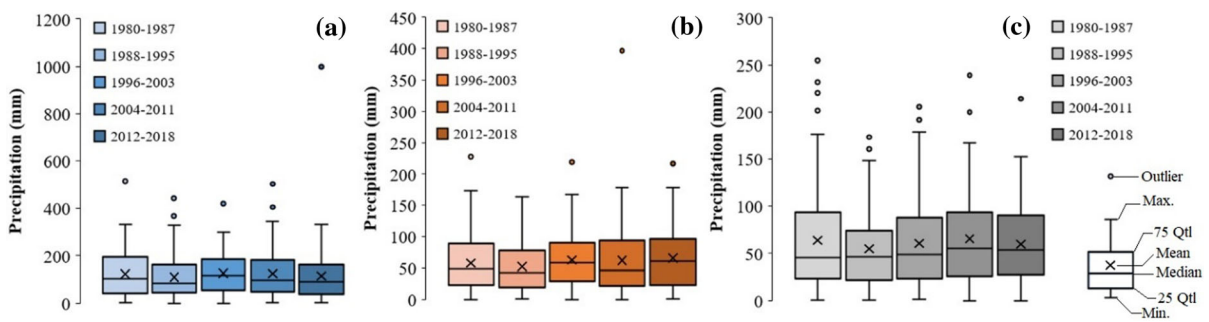

Figure 4
Changes in the distribution of precipitation time series at **a** ULU, **b** OSM, and **c** KEL stations

and KEL are expected to have similarities, which are examined in the subsequent sections.

The SPI time series considering a 48-MA at ULU station indicated a wet period in early 2015 followed by a decline after the year 2016 (Fig. 5a) that turned to be the worst drought event in recent years (after 2017). Based on Fig. 5c and e, a spike followed by a mild decline occurred in both KEL and OSM in early 2010, while the nature of the SPI time series in OSM depicted more oscillatory between wet and dry spells. On the other hand, when the previous SPI terms are evaluated, the recent values of 48-month SPI could be interpreted as natural dry and wet cycles in the region. Particularly, the deficit of the recent years could be a drawback for the surplus between 2015 and 2017 years which is milder in the magnitude. Although WD confirms the results of SPI, the pieces of evidence are not adequate to confidently link the recent droughts to climate change. The same results are observed at an annual scale (Fig. 5b), but the MA component with a 48-month lag in Fig. 5a showed more transparent results. Accordingly, the late 2015 decline could be a long-lasting drought at the summit.

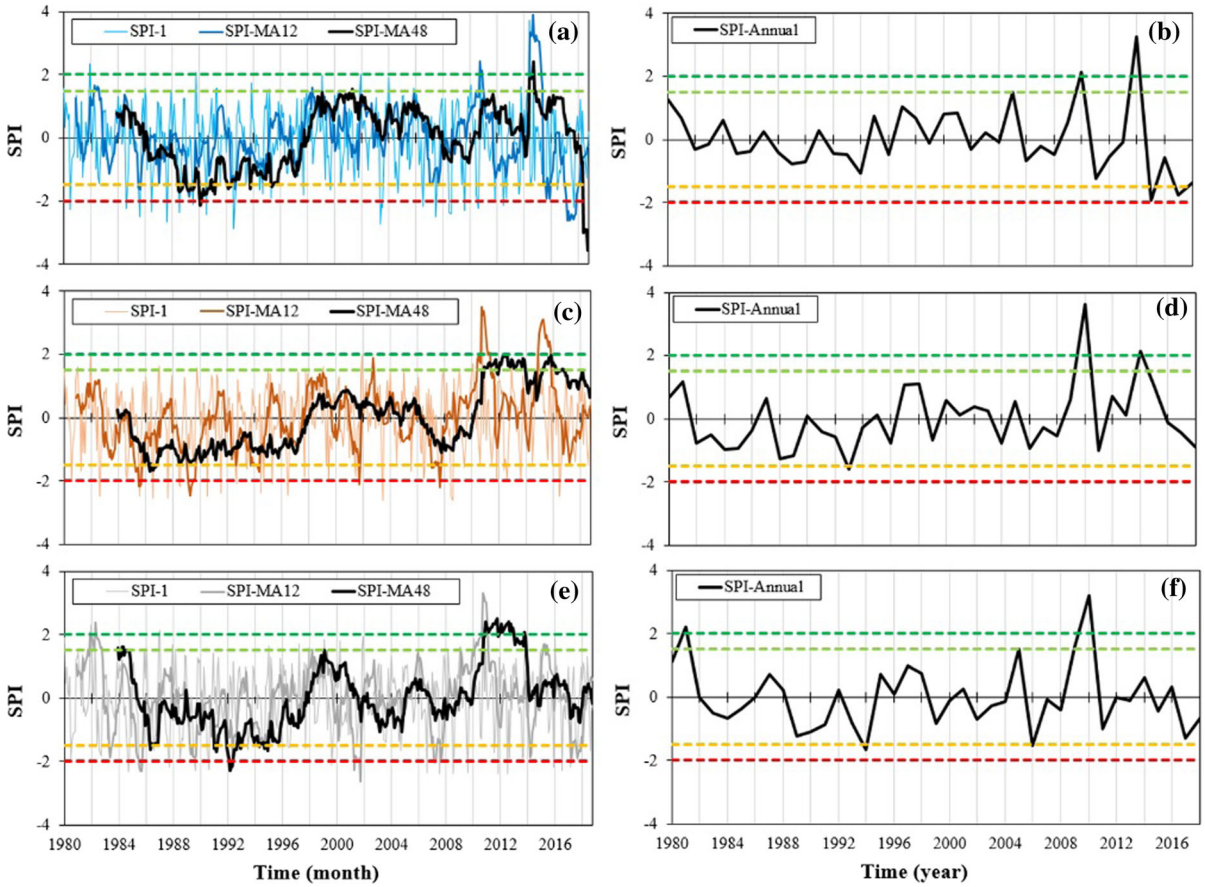

Figure 5
Results of SPI analysis in **a**, **b** ULU, **c**, **d** OSM, and **e**, **f** KEL stations. The dashed lines indicate the SPI evaluation criteria of extreme wet, very wet, severely dry, and extremely dry from up to down, respectively, which is detailed previously in Table 2

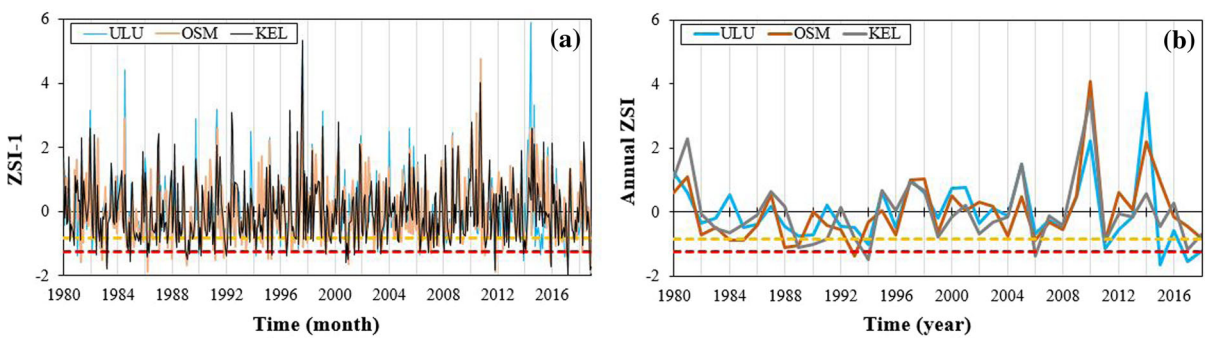

Figure 6
Results of ZSI analysis on the precipitation time series at **a** monthly and **b** annual scale

For further investigation of the drought patterns, the monthly and annual ZSI was also evaluated, as shown in Fig. 6. The ZSI values on a monthly scale are more or less similar to those obtained by the SPI on a monthly scale. This is because of the similar methodology that SPI and ZSI share. Additionally,

the ZSI-1 index showed several passes from the evaluation criteria, whilst the SPI-1 showed oscillations within the limits, which suggests the superiority of ZSI over SPI. Therefore, SPI is more useful in identifying long-term drought through the application of MA in the analysis. The same results were obtained at an annual scale (Fig. 6b) for all of the stations, which is very similar to those of SPI in Fig. 5b. Consequently, based on ZSI, the recent droughts are not so different from the historical events in the region.

The results of MCZI and RAI at a monthly scale are given in Fig. 7. The results of the MCZI resemble the SPI-1 values, while the value obtained for RAI is more like the ZSIs. The difference between the SPI and ZSI methodologies increases when considering additional RAI and MCZI. In this respect, the best sign of drought is depicted by the MCZI, which is similar to that of ZSI. Since these indices are usually evaluated on a monthly scale, the MCZI and RAI are used to evaluate the SPI-1 and ZSI-1 results only. Hence, it can be concluded that the large-scale decline defined by the WD could be depicted by the SPI within the context of MA-48. At the monthly scale, the most effective indexes are found to be ZSI and MCZI, based on the depiction of the same decline as revealed by WD in pattern recognition. On the other hand, when the MA component is used, SPI showed superior abilities in evaluating the drought patterns over several months. However, the criteria used in SPI analysis showed more informative details about the degree of severity in the wet and dry spells of the region. It is worth noting that the application of the modified RAI in practice (e.g. Hansel et al., 2016; Mutti et al., 2020) would provide better drought projection, similar to SPI, when the scaling factor or intensity duration frequency (IDF) curves in the region are available.

5. Discussion

This study aimed to take a deeper look at the drought phenomenon by comparing the signal analysis and drought indices. It is important to recognize that the initiation of drought can be based on a simple precipitation time series and the associated signal processing.

In the data analysis, the oscillatory nature of the phenomenon was linked to the natural repeating pattern in the time series. This can be interpreted as the consequences of large-scale atmospheric oscillation such as the North Atlantic Oscillation (NAO), El Niño/Southern Oscillation (ENSO), Atlantic Multi-Decadal Oscillation (AMO), and Pacific Decadal Oscillation (PDO). A similar analysis can be conducted by evaluating the time series of the large-scale oscillation and precipitation patterns at a similar or lagged time window (e.g. Vaheddoost, 2017). On the other hand, the behavior of the phenomenon indicated a low persistence in the data run. Although it is expected behavior for a precipitation time series, the degree of persistence and increase in decay varied based on the regional climate. In particular, for the case of Uludag, a 3-month persistence based on MI and ACF on a monthly scale is quite long-lasting and

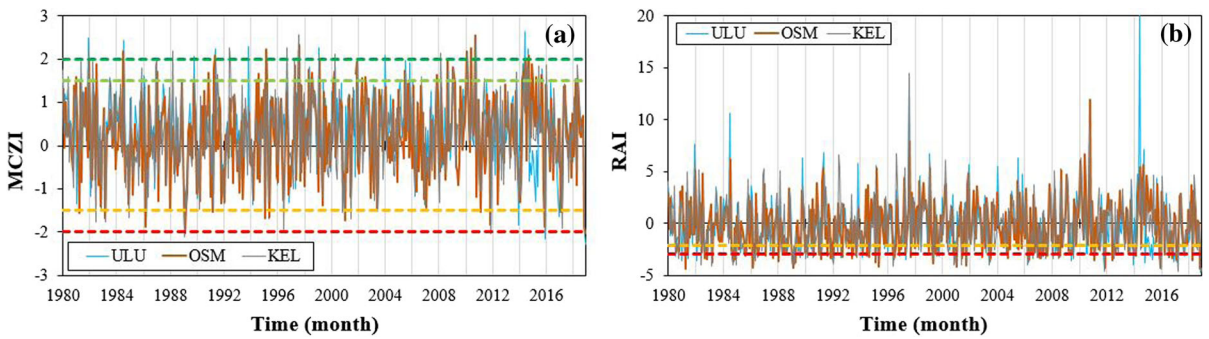

Figure 7
Results of MCZI and RAI at monthly scale

indicates stable climate behavior. This is confirmed by the power spectrum analysis in which several seasonality patterns emerged. However, the decomposition of the precipitation signal indicated an obvious decline associated with large repeating patterns (at 1, 3, 5, 6, 12, 22, and 60 months). This was accepted as a major drought pattern and interpreted with the less frequent precipitation events when compared to the historical records.

The drought components showed that the sinusoidal pattern of the precipitation at the summit is disturbed but does not necessarily show a long-lasting drought. It was found that the drought pattern at the summit (ULU stations) extends toward the southern hillside in Keles. The WD harmonic components showed similarities to the results obtained by Vaheddoost (2020b). It was found that the decline is more likely due to climate variability than climate change. Hence, results of the drought analysis in ULU station are in agreement with the studies of Sen (2013), Sirdas and Sen (2003), and Simisek and Cakmak (2010). The distribution of the precipitation become more platykurtic, which is linked to the less frequent events. This was found to be a sign of less frequent events, which was addressed by Vaheddoost (2020b), but could not be interpreted as a clear sign of a continuous trend in the data run. In addition, SPI analysis in Fig. 5a confirms the results of Vaheddoost (2019), who monitored short-term declines in the precipitation time series at the Uludag station. The application of the drought indices showed that the moving average component in the analysis is an inseparable part of the study, and in particular for the case of Uludag station, it indicates an ongoing drought event. When the long-term drought patterns were investigated, the added value provided by the MA component is very useful. The difference between the results obtained by each index is due to the mathematical application and the methodology, which reveals a different aspect of drought pattern in the time series.

The recent drought pattern depicted by the MA-48 time frame indicates a long-lasting drought that could trigger wildfires in the forest and a shortage in snowpack reserves. Regardless of the obtained results, further spatiotemporal investigation is needed to ensure the results in practice. The limitation of this study, however, is the consideration of other climatic variables such as temperature, evaporation, albedo, and in situ measurements. In some indices such as RAI, a scaling factor such as those used in the modified RAI may reveal more realistic results. The ensemble of the climate-born events including general circulation models (GCMs) under the representative concentration pathway (RCP) scenarios and their effect on drought patterns can be investigated in detail. One may also use more sophisticated drought indices such as SPEI, reclamation drought index (RDI), water supplying vegetation index (WSVI), or modified RAI when critical information about the scaling factor, IDF curves, and climatic behavior of the region are available. The superiority of the SPI with MA-48 over the other indices should be examined through a careful extension of the analysis to other regions. As results indicate the effect of large-scale oscillations, phenomena such as climate change and climate variability should also be investigated more precisely. For this, the cross-wavelet analysis and other signal decomposition methods are suggested for further investigation.

6. Conclusions

Bursa is an important hub for the agro-food security of Turkey. In this respect, Uludag, as one of the main features that affect the hydrology of the region, is addressed. Monthly precipitation at the summit of Mount Uludag and hillsides is analyzed using signal analysis (AC, PAC, MI, PS, and WD) and several drought indices (SPI, ZSI, MCZI, and RAI) to investigate the drought in a mountainous region. The following conclusions are made:

1- There are significant large-scale repeating cycles at 1, 3, 5, 6, 12, 22, and 60 months which are linked to the climate variability.
2- Results of the WD showed that there is a decline in the large-scale cycles of the precipitation time series which was not observed within the past 39 years. Particularly at the summit and southern hillside, a drop in long-term precipitation time series occurred.

3- The most effective drought indexes at the monthly scale were found to be ZSI and MCZI. However, when the MA term was used, SPI was found to be more transparent.
4- Based on the results, the most severe droughts at the summit have taken place in recent years, following by a wet period in early 2015, and this may have triggered wildfires and degradation of snowpack in the region.
5- It was concluded that this evidence does not necessarily indicate human-induced climate change in the region, and declines instead seem to be a product of climate variability.
6- Further investigation is needed considering recent precipitation records and other climatic variables, as well as in situ measurements, to obtain more applicable results.

Declarations

Conflict of interest The authors declare that they have no conflict of interest.

Publisher's Note Springer Nature remains neutral with regard to jurisdictional claims in published maps and institutional affiliations.

References

Abramowitz, M., & Stegun, I. A. (Eds.). (1970). *Handbook of mathematical functions with formulas, graphs, and mathematical tables*. (Vol. 55)US Government Printing Office.

Afshar, M. H., Sorman, A. U., Tosunoglu, F., Bulut, B., Yilmaz, M. T., & Mehr, A. D. (2020). Climate change impact assessment on mild and extreme drought events using copulas over Ankara, Turkey. *Theoretical and Applied Climatology, 26*(2), 254–268

AgriMetSoft. (2017). Meteorological drought monitor (Version 1) [Computer software]. https://agrimetsoft.com/MDM.aspx. Accessed September 2019

Aladaileh, H., Al Qinna, M., Karoly, B., Al-Karablieh, E., & Rakonczai, J. (2019). An investigation into the spatial and temporal variability of the meteorological drought in Jordan. *Climate, 7*(6), 82

Azmi, M., Rüdiger, C., & Walker, J. P. (2016). A data fusion-based drought index. *Water Resources Research, 52*(3), 2222–2239

Bahrami, M., Bazrkar, S., & Zarei, A. R. (2019). Modeling, prediction and trend assessment of drought in Iran using standardized precipitation index. *Journal of Water and Climate Change, 10*(1), 181–196

Bhalme, H. N., & Mooley, D. A. (1980). Large-scale droughts/floods and monsoon circulation. *Monthly Weather Review, 108*(8), 1197–1211

Caloiero, T., & Veltri, S. (2019). Drought assessment in the Sardinia Region (Italy) during 1922–2011 using the standardized precipitation index. *Pure and Applied Geophysics, 176*(2), 925–935

Cavus, Y., & Aksoy, H. (2019). Spatial drought characterization for Seyhan River basin in the Mediterranean region of Turkey. *Water, 11*(7), 1331

Craig, C. A., Allen, M. W., Feng, S., & Spialek, M. L. (2020). Exploring the impact of resident proximity to wildfires in the northern Rocky Mountains: Perceptions of climate change risks, drought, and policy. *International Journal of Disaster Risk Reduction, 44*, 101420

Du, J., Fang, J., Xu, W., & Shi, P. (2013). Analysis of dry/wet conditions using the standardized precipitation index and its potential usefulness for drought/flood monitoring in Hunan Province, China. *Stochastic Environmental Research and Risk Assessment, 27*(2), 377–387

Edwards, D. C., & McKee, T. B. (1997). *Characteristics of 20th century drought in the United States at multiple time scales: Atmospheric science paper no. 634*. (pp. 1–30). Colorado State University.

Eris, E., Cavus, Y., Aksoy, H., Burgan, H. I., Aksu, H., & Boyacioglu, H. (2020). Spatiotemporal analysis of meteorological drought over Kucuk Menderes River Basin in the Aegean Region of Turkey. *Theoretical and Applied Climatology, 142*(3), 1515–1530

Eslamian, S. (Ed.). (2014). *Handbook of engineering hydrology: modeling, climate change, and variability*. CRC Press.

Gao, L., & Zhang, Y. (2016). Spatio-temporal variation of hydrological drought under climate change during the period 1960–2013 in the Hexi Corridor, China. *Journal of Arid Land, 8*(2), 157–171

Gibbs, W. J., & Maher, J. V. (1967). Rainfall deciles as drought indicators. Bureau of Meteorology Bulletin No. 48. Commonwealth of Australia, Melbourne

Gray, R. M. (1990). *Entropy and information theory*. Springer.

Hansel, S., Schucknecht, A., & Matschullat, J. (2016). The Modified Rainfall Anomaly Index (mRAI)—is this an alternative to the Standardised Precipitation Index (SPI) in evaluating future extreme precipitation characteristics? *Theoretical and Applied Climatology, 123*(3–4), 827–844

Hao, Z., & Singh, V. P. (2015). Drought characterization from a multivariate perspective: A review. *Journal of Hydrology, 527*, 668–678

Hao, Z., Hao, F., Singh, V. P., Ouyang, W., Zhang, X., & Zhang, S. (2020). A joint extreme index for compound droughts and hot extremes. *Theoretical and Applied Climatology*, *142*(1), 321–328

Hao, X., Ma, H., Hua, D., Qin, J., & Zhang, Y. (2019). Response of ecosystem water use efficiency to climate change in the Tianshan Mountains, Central Asia. *Environmental monitoring and assessment, 191*(9), 561

Jasim, A. I., & Awchi, T. A. (2020). Regional meteorological drought assessment in Iraq. *Arabian Journal of Geosciences, 13*(7), 1–16

Ju, X. S., Yang, X. W., Chen, L. J., & Wang, Y. M. (1997). Research on determination of indices and division of regional flood/drought grades in China. *Quarterly Journal of Applied Meteorology, 8*(1), 26–33 In Chinese.

Kashyap, R. L., & Rao, A. R. (1976). *Dynamic stochastic models from empirical data*. Academic Press.

Katip, A. (2018). Meteorological drought analysis using artificial neural networks for Bursa City, Turkey. *Applied Ecology and Environmental Research, 16*(3), 3315–3332

Li, L., She, D., Zheng, H., Lin, P., & Yang, Z. L. (2020). Elucidating diverse drought characteristics from two meteorological drought indices (SPI and SPEI) in China. *Journal of Hydrometeorology, 21*(7), 1513–1530

McKee, T. B., Doesken, N. J., & Kleist, J. (1995). Drought monitoring with multiple-time scales. In: Preprints ninth conference on applied climatology. American Meteorological Society, Boston, pp. 233–236.

Mehdizadeh, S., Ahmadi, F., Mehr, A. D., & Safari, M. J. S. (2020). Drought modeling using classic time series and hybrid wavelet-gene expression programming models. *Journal of Hydrology, 587*, 125017

Mehr, A. S., Safari, M. J. S., & Nourani, V. (2021). Wavelet packet-genetic programming: a new model for meteorological drought hindcasting. *Teknik Dergi*. https://doi.org/10.18400/tekderg.605453

Meyer, Y. (1992). *Wavelets and operators*. Cambridge University Press. ISBN 0-521-42000-8.

Mohammadi, B., Vaheddoost, B., & Mehr, A. D. (2020). A spatiotemporal teleconnection study between Peruvian precipitation and oceanic oscillations. *Quaternary International*. https://doi.org/10.1016/j.quaint.2020.09.042

Mohammed, S., Alsafadi, K., Al-Awadhi, T., Sherief, Y., Harsanyie, E., & El Kenawy, A. M. (2020). Space and time variability of meteorological drought in Syria. *Acta Geophysica, 68*(6), 1877–1898

World Meteorological Organization (WMO) (2011). Proceedings of an expert meeting. 2–4 June, 2010, Murcia, Spain.

Mutti, P. R., de Abreu, L. P., de Andrade, M. B. L., Spyrides, M. H. C., Lima, K. C., de Oliveira, C. P., Dubreuil, V., & Bezerra, B. G. (2020). A detailed framework for the characterization of rainfall climatology in semiarid watersheds. *Theoretical and Applied Climatology, 139*(1), 109–125

Ozturk, M. (2010). Uludağ (Zirve) ve Bursa Meteoroloji İstasyonlarının Karşılaştırmalı İklimi. *Türk Coğrafya Dergisi, 55*, 13–24 (in Turkish).

Rader, C., & Brenner, N. (1976). A new principle for fast Fourier transformation. *IEEE Transactions on Acoustics, Speech, and Signal Processing, 24*(3), 264–266

Rashid, M. M., & Beecham, S. (2019). Development of a non-stationary Standardized Precipitation Index and its application to a South Australian climate. *Science of the Total Environment, 657*, 882–892

Salas, J. D., Delleur, V., Yevjevich, V., & Lane, W. L. (1980). *Applied modeling of hydrologic time series*. Water Resources Publication.

Sen, Z. (2013). Square diagonal trend test procedure. In: 6th international perspective on water resources and the environment, January, 07-09. Izmir, Turkey

Sen, B., Topcu, S., Türkeş, M., Sen, B., & Warner, J. F. (2012). Projecting climate change, drought conditions and crop productivity in Turkey. *Climate Research, 52*, 175–191

Sepulcre-Canto, G., Horion, S. M. A. F., Singleton, A., Carrao, H., & Vogt, J. (2012). Development of a combined drought indicator to detect agricultural drought in Europe. *Natural Hazards and Earth System Sciences, 12*(11), 3519–3531

Shannon, C. E., & Weaver, W. (1949). *The mathematical theory of communication*. University of Illinois Press.

Sharafati, A., Nabaei, S., & Shahid, S. (2020). Spatial assessment of meteorological drought features over different climate regions in Iran. *International Journal of Climatology, 40*(3), 1864–1884

Simisek, O., & Cakmak, B. (2010). Drought analysis for 2007–2008 agricultural year of Turkey. *Tekirdağ Ziraat Fakültesi Dergisi, 7*(3), 99–109

Sirdas, S., & Sen, Z. (2003). Spatio-temporal drought analysis in the Trakya region, Turkey. *Hydrological Sciences Journal, 48*(5), 809–820. https://doi.org/10.1623/hysj.48.5.809.51458

Starks, P. J., Steiner, J. L., Neel, J. P., Turner, K. E., Northup, B. K., Gowda, P. H., & Brown, M. A. (2019). Assessment of the Standardized Precipitation and Evaporation Index (SPEI) as a potential management tool for grasslands. *Agronomy, 9*(5), 235

Sun, C. X., Huang, G. H., Fan, Y., Zhou, X., Lu, C., & Wang, X. Q. (2019). Drought occurring with hot extremes: Changes under future climate change on Loess Plateau, China. *Earth's Future, 7*(6), 587–604

Tatli, H. (2015). Downscaling standardized precipitation index via model output statistics. *Atmósfera, 28*(2), 83–98. https://doi.org/10.1016/S0187-6236(15)30002-3

Turkes, M. (2020). Climate and drought in Turkey. *Water resources of Turkey*. (pp. 85–125). Springer.

Turkes, M., Telat, K. O. C., & Saris, F. (2007). Türkiye'nin Yağiş Toplami ve Yoğunluğu Dizilerindeki Değişikliklerin ve Eğilimlerin Zamansal ve Alansal Çözümlemesi. *Cografi Bilimler Dergisi, 5*(1), 57–73 In Turkish.

Vaheddoost, B. (2017). Spatial analysis of large atmospheric oscillations and annual precipitation in Lake Urmia Basin. *European Water, 59*, 123–129

Vaheddoost, B. (2020b). A comparative determination of the monthly precipitations trends in Bursa, Turkey. *Uludağ University Journal of The Faculty of Engineering, 25*(1), 153–168

Vaheddoost, B. (2020a). A spatiotemporal classification of the peruvian precipitations between 1990 and 2015. *Pure and Applied Geophysics, 177*(9), 4509–4520

Vaheddoost, B. (2019). Evaluation of monthly drought using Standardized Precipitation Index in Bursa, Turkey. In: 4th Eurasian conference on civil and environmental engineering (ECOCEE), June 17–18, DoubleTree by Hilton, Istanbul, Turkey.

Van Rooy, M. P. (1965). A Rainfall Anomaly Index independent of time and space. *Notos, 14*, 43–48

Vicente-Serrano, S. M., Beguería, S., & López-Moreno, J. I. (2010). A multiscalar drought index sensitive to global warming: The standardized precipitation evapotranspiration index. *Journal of Climate, 23*(7), 1696–1718

Wilhite, D. A., & Glantz, M. H. (1985). Understanding: The drought phenomenon: The role of definitions. *Water International, 10*(3), 111–120

Willeke, G., Hosking, J. R. M., Wallis, J. R., & Guttman, N. B. (1994). The national drought atlas. Institute for Water Resources Report 94-NDS-4, U.S. Army Corps of Engineers

Wilson, E. B., & Hilferty, M. M. (1931). The distribution of chi-square. *Proceedings of the National Academy of Sciences of the United States of America, 17*, 684–688

Yihdego, Y., Webb, J., & Vaheddoost, B. (2017). Highlighting the role of groundwater in lake–aquifer interaction to reduce vulnerability and enhance resilience to climate change. *Hydrology, 4*(1), 10

Yihdego, Y., Vaheddoost, B., & Al-Weshah, R. A. (2019). Drought indices and indicators revisited. *Arabian Journal of Geosciences, 12*(3), 69

Yilmaz, E. (2018). Türkiye'de aylık yağış eğilimleri, yağış kaymaları ve yağış Eğilim Rejimleri (1971–2010) (monthly precipitation trends, precipitation temporal shifts and precipitation trends regimes in Turkey (1971–2010)). *Journal of Human Sciences, 15*(4), 2066–2091. https://doi.org/10.2139/ssrn.3419380

Zhou, J., Li, Q., Wang, L., Lei, L., Huang, M., Xiang, J., Feng, W., Zhao, Y., Xue, D., Liu, C., Wei, W., & Zhu, G. (2019). Impact of climate change and land-use on the propagation from meteorological drought to hydrological drought in the eastern Qilian Mountains. *Water, 11*(8), 1602

Zhu, G. F., Yang, L., Qin, D. H., Tong, H. L., Liu, Y. F., & Li, J. F. (2016). Spatial and temporal variation of drought index in a typical steep alpine terrain in Hengduan Mountains. *Journal of Mountain Science, 13*(7), 1186–1199

(Received June 30, 2020, revised April 5, 2021, accepted April 17, 2021, Published online May 7, 2021)